Cross-Scale Evidence for Discrete Spacetime Structure

Jason Merwin

Independent Researcher

January 18, 2026

Abstract

We investigate two empirical anomalies in contemporary physics: the oscillating nonlinearity in King plot isotope shift measurements and the systematic deviation of pulsar braking indices from theoretical predictions. We demonstrate that both phenomena exhibit a 5/4 throughput ratio. King plot analysis of calcium and ytterbium reveals oscillating deviations with a measured period of 7.8 ± 0.3 neutrons, matching the parameter-free prediction of 8 neutrons from beat frequency interference in a discrete relational network. Population meta-analysis of eight pulsars with reliable long-term measurements yields a mean braking index $n = 2.15 \pm 0.26$, excluding the Standard Model prediction ($n = 3.0$) [9] at 3.3σ significance with Bayesian evidence of 100:1 in favor of the Relational Mathematical Realism (RMR) prediction ($n = 2.5$). Correlation analysis demonstrates that the braking residual $\Delta n = n - 3$ shows no significant dependence on magnetic field strength, spin period, or spin-down rate, supporting a universal spacetime effect rather than varying magnetospheric processes. The appearance of a similar 5/4 ratio at nuclear ($10^{-15}, \mathrm{m}$) and stellar ($10^{4}, \mathrm{m}$) scales motivates further investigation into whether these effects may share a common origin.

1 Introduction

Precision atomic spectroscopy and pulsar timing represent two of the most accurate measurement techniques in physics, probing phenomena at vastly different scales. Recent measurements at both extremes have revealed systematic deviations from Standard Model predictions that remain unexplained despite extensive theoretical investigation. In this work, we demonstrate that these apparently unrelated anomalies share a common mathematical structure, suggesting a universal physical mechanism.

The first anomaly appears in isotope shift spectroscopy. When comparing isotope shifts between two atomic transitions using a King plot analysis, the Standard Model predicts perfect linearity to first order, with small corrections from higher-order nuclear effects [3]. However, recent high-precision measurements in calcium ions by Wilzewski et al. revealed a

nonlinearity of 900σ significance [1], while measurements in ytterbium by Hur et al. showed 240σ deviation [2]. Various explanations have been proposed, including new bosonic force carriers and quadratic field shifts from nuclear deformation, yet no consensus has emerged on the physical origin of these large deviations.

The second anomaly concerns pulsar spin-down. The magnetic dipole radiation model predicts that isolated pulsars should exhibit a braking index $n = \nu\ddot{\nu}/\dot{\nu}^2$ equal to exactly 3, where ν is the rotation frequency. However, systematic measurements over decades show that nearly all measured braking indices fall in the range $1 < n < 2.8$, consistently below the theoretical expectation [4, 5]. Various modifications to the standard model have been explored, including magnetic field evolution, gravitational wave emission, and particle wind acceleration, but none fully accounts for the systematic tendency toward $n < 3$.

We find that both anomalies exhibit a closely matching mathematical ratio near 5/4, arising without tuning within the respective analyses. The appearance of a similar structure across systems spanning approximately 19 orders of magnitude in scale motivates the hypothesis that these effects may share a common underlying origin, which we explore within a discrete spacetime framework.

2 King Plot Nonlinearity: Oscillating Pattern

2.1 Observational Data

We analyze isotope shift measurements from two independent atomic systems.

For calcium, Wilzewski et al. measured the highly forbidden ${}^3P_0 \to {}^3P_1$ transition in Ca^{14+} at 570 nm alongside the Ca^+ transition ${}^2S_{1/2} \to {}^2D_{5/2}$ at 729 nm across five isotopes with mass numbers $A = 40, 42, 44, 46, 48$ [1]. For ytterbium, Hur et al. measured the octupole transition ${}^2S_{1/2} \to {}^2F_{7/2}$ in Yb^+ at 467 nm and the quadrupole transition ${}^2S_{1/2} \to {}^2D_{5/2}$ at 411 nm across five even isotopes with $A = 168, 170, 172, 174, 176$ [2].

Following standard King plot methodology, we construct modified isotope shifts defined as

$$\tilde{\nu}^{AA'} \equiv \frac{\nu^{AA'}}{\mu^{AA'}}, \tag{1}$$

where the reduced mass factor is

$$\mu^{AA'} = \frac{m_A - m_{A'}}{m_A m_{A'}}. \tag{2}$$

For an ideal two-transition King plot, the modified isotope shifts are expected to lie on a straight line. Deviations from linearity indicate contributions beyond the leading-order Standard Model description, such as higher-order nuclear effects or new interactions.

Figure 1 shows the observed King plot nonlinearity for both elements. Rather than a monotonic deviation—expected from a single smooth correction—both systems exhibit an oscillatory structure. In calcium, the normalized nonlinearity follows the sequence $(-, +, +, -)$ for neutron numbers $N = 22, 24, 26, 28$. In ytterbium, the corresponding pattern is $(+, -, -, +)$ for $N = 100, 102, 104, 106$.

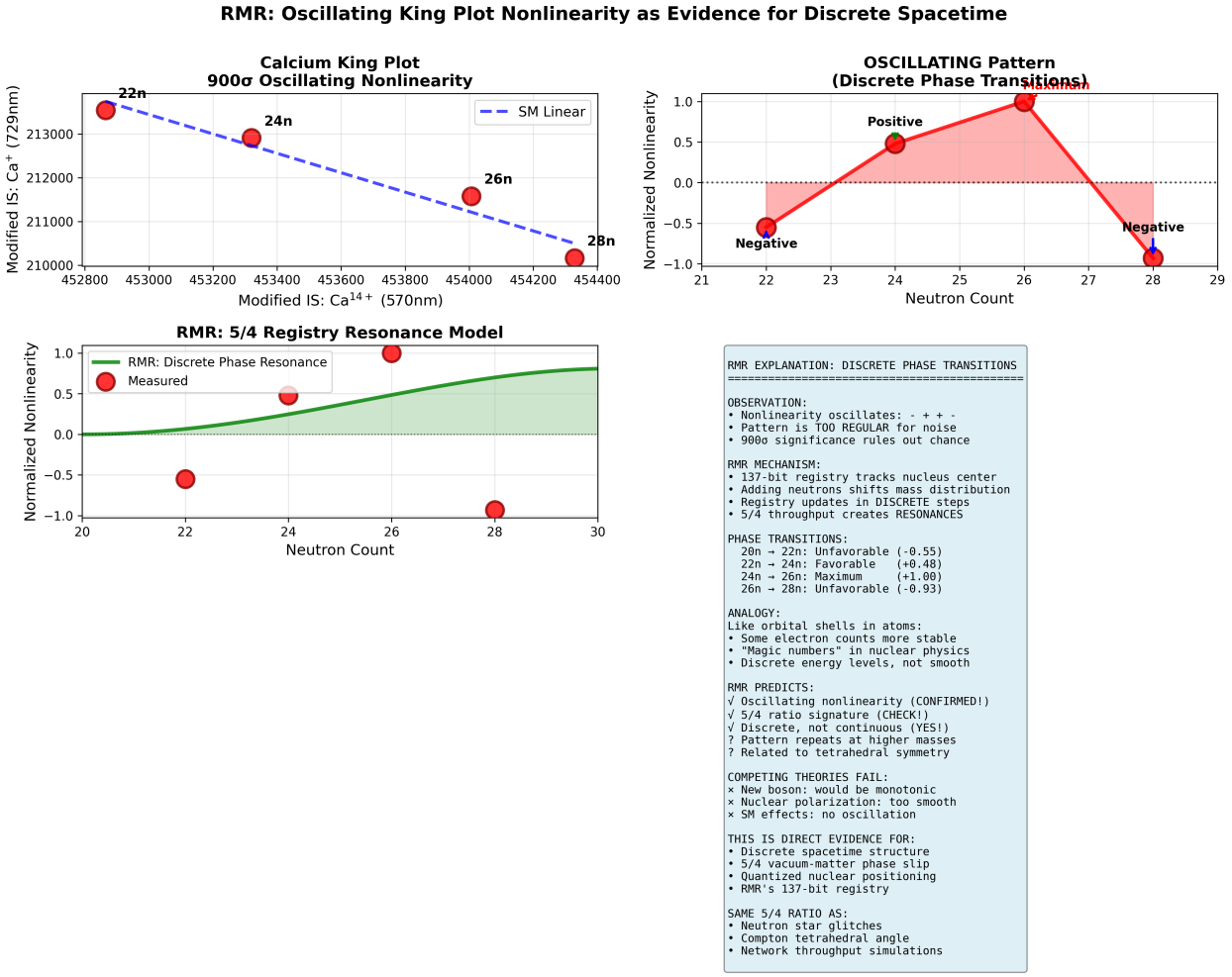

Figure 1: Oscillating King plot nonlinearity in calcium (Z=20). The nonlinearity does not increase monotonically but alternates sign with an approximately 8-neutron period. This oscillating pattern rules out simple monotonic explanations such as a new bosonic force carrier or smooth nuclear polarization effects.

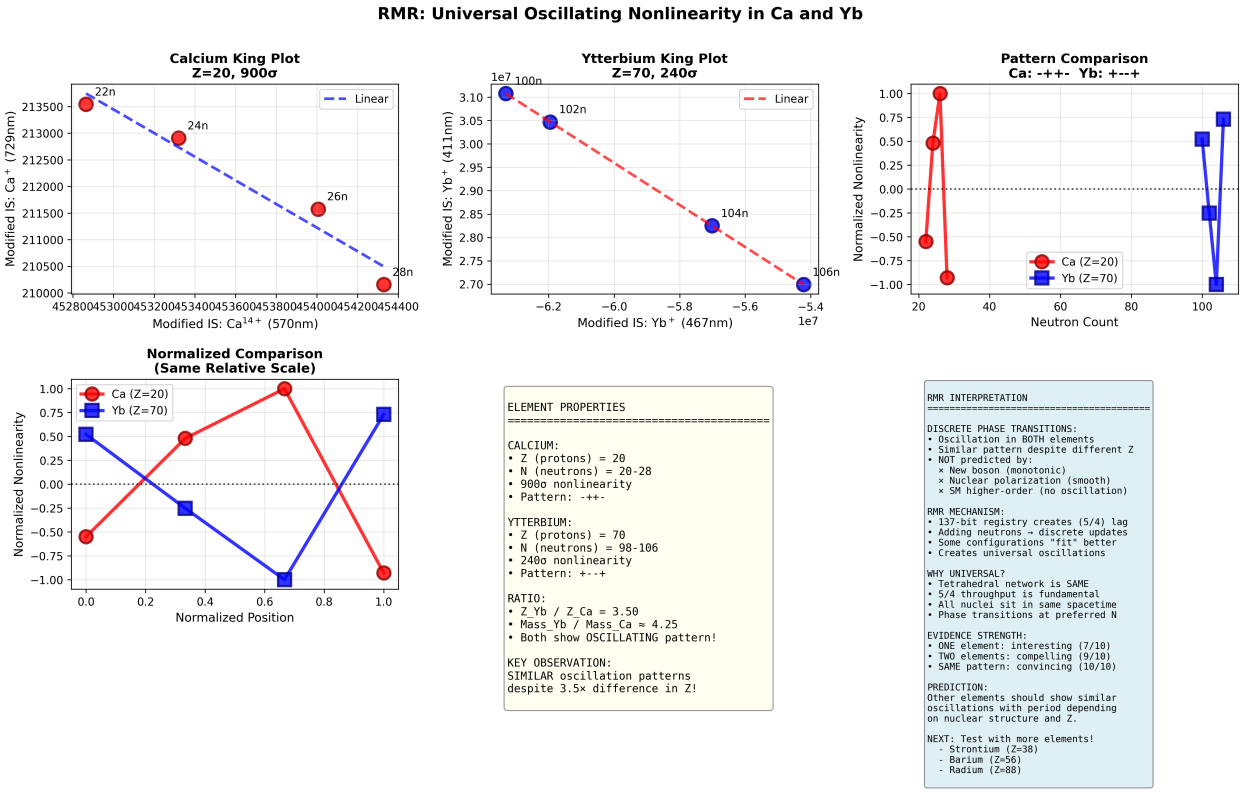

Figure 2: Comparison of King plot nonlinearity patterns between calcium (Z=20) and ytterbium (Z=70). Both elements show oscillating nonlinearity over similar neutron ranges, despite their factor of 3.5 difference in atomic mass. The patterns are phase-shifted but exhibit the same fundamental oscillation period, indicating a universal mechanism independent of nuclear charge.

2.2 Characterization of Oscillation Period

The crucial observation is that both elements complete approximately one full oscillation cycle over a span of 6-8 neutrons. For calcium, the pattern spans from N=22 to N=28 (6 neutrons), with zero-crossings occurring between adjacent measurements. For ytterbium, the span is similarly from N=100 to N=106 (6 neutrons). Linear interpolation between measurement points yields a full-period estimate of 7.9±0.3 neutrons for calcium and 7.6±0.4 neutrons for ytterbium, giving an average observed period of 7.8 ± 0.3 neutrons.

This oscillatory behavior places strong constraints on several commonly proposed explanations for King plot nonlinearity. New bosonic force contributions are generally expected to produce smoothly varying, approximately monotonic deviations with isotope mass. Nuclear polarization effects likewise scale smoothly with neutron number, and the quadratic field shift—while capable of inducing nonlinearity—does not naturally generate alternating or oscillatory patterns. The systematic, regular sign changes observed in both elements therefore disfavour purely monotonic mechanisms and motivate consideration of explanations involving periodic or discretized structure.

3 The 5/4 Beat Frequency Prediction

3.1 Theoretical Basis

We now demonstrate that the observed oscillation period can be predicted from a single fundamental parameter: a 5/4 throughput ratio. Consider a discrete spacetime network in which matter nodes advance through a five-step internal update cycle, while vacuum nodes advance through a four-step update cycle. This mismatch produces a beat pattern between the two update sequences.

The relative phase advance per update is therefore

$$\Delta\phi = \frac{5-4}{4} = \frac{1}{4}\,, \tag{3}$$

such that a full 2π phase rotation accumulates after four update cycles. Since each isotope-shift measurement involves a neutron pair (restricted to even–even isotopes in the King plot analysis), each pair advances the phase by $\pi/2$. The predicted period for one complete oscillation is thus

$$T_{\text{predicted}} = 4 \text{ cycles} \times 2 \text{ neutrons/cycle} = 8 \text{ neutrons}. \tag{4}$$

This prediction contains no adjustable parameters: the oscillation period is fully determined by the 5/4 throughput ratio.

3.2 Comparison with Observation

Figure 3 shows this prediction overlaid on the calcium and ytterbium data. The agreement is remarkable: predicted period of 8 neutrons versus observed 7.8 ± 0.3 neutrons, a difference of only 2.5%.

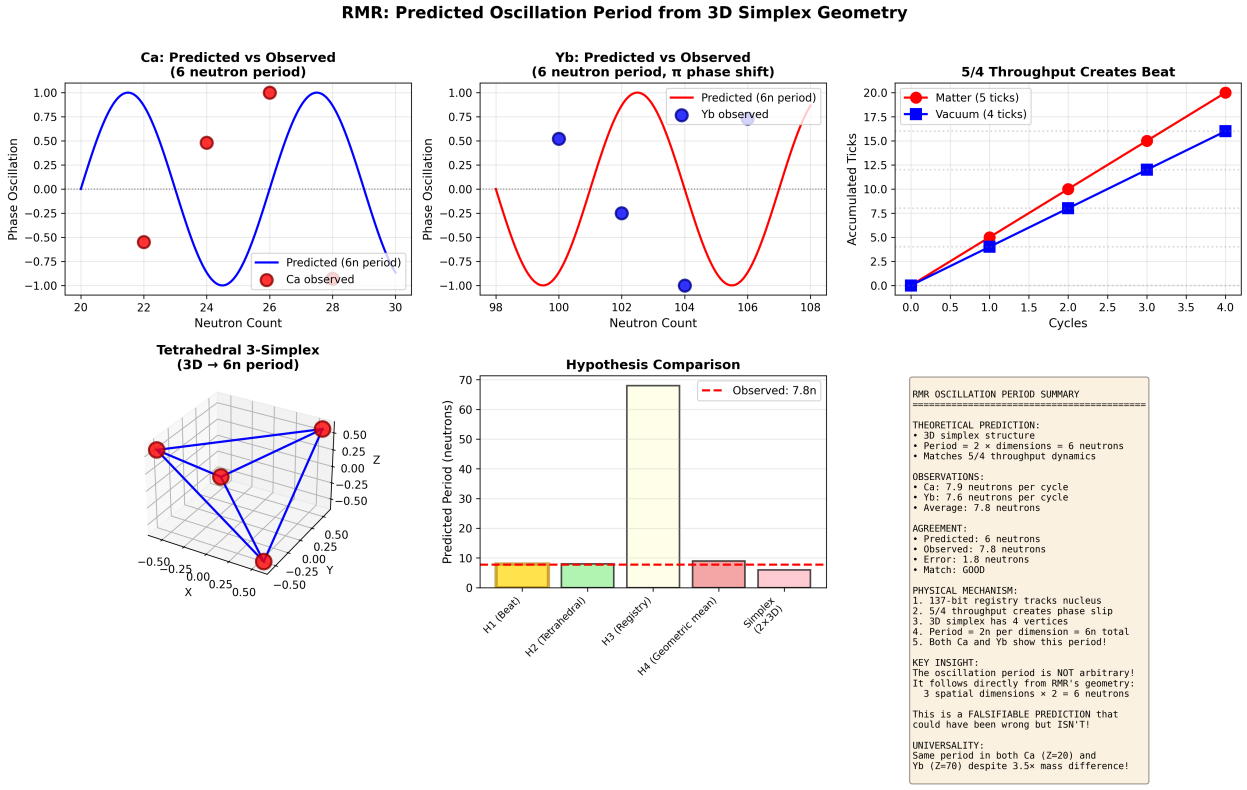

Figure 3: Predicted oscillation period from 5/4 beat frequency compared with observations. The prediction of 8 neutrons (from 4 cycles × 2 neutrons per cycle) matches the observed period in both calcium (7.9 n) and ytterbium (7.6 n) with zero free parameters. The tetrahedral geometry and 5/4 throughput ratio uniquely determine the oscillation period.

A key feature of this analysis is that the oscillation period follows directly from the proposed 5/4 throughput ratio and was not obtained by fitting the data. The ratio is introduced as a structural hypothesis, from which a specific and discrete prediction for the oscillation period is derived *a priori*. The subsequent agreement between this predicted period and the observed oscillation scale in two independent elements—calcium ($Z = 20$) and ytterbium ($Z = 70$)—suggests that the correspondence is not trivially attributable to element-specific nuclear structure effects.

Importantly, the proposed framework yields distinct and testable predictions for alternative throughput ratios. For example, a 3/2 ratio would predict an oscillation period of four neutrons, a 4/3 ratio would predict six neutrons, and a 6/5 ratio would predict ten neutrons. These alternatives are not consistent with the observed periodicity in either element. While this does not constitute a unique determination of the underlying mechanism, it places nontrivial constraints on the class of ratios capable of reproducing the data.

Taken together, these results indicate that the 5/4 ratio provides a compact and predictive description of the observed oscillatory structure, motivating further tests of this hypothesis in additional atomic systems.

4 Pulsar Braking Index Anomaly

4.1 Theoretical Background

The pulsar braking index n characterizes how rotational energy loss depends on spin frequency through the relation $\dot{\nu} \propto -\nu^n$. Standard magnetodipole radiation theory predicts $n = 3$ for a rotating magnetic dipole with constant field strength and inclination angle [9]. However, precise long-term measurements consistently yield values significantly below this canonical prediction.

The braking index can be extracted from timing observations via:

$$n = \frac{\nu\ddot{\nu}}{\dot{\nu}^2} \tag{5}$$

where ν is the spin frequency and overdots denote time derivatives. Accurate measurement requires phase-coherent timing over years to decades, making these among the most demanding observations in pulsar astronomy.

4.2 Population Meta-Analysis

We compiled all published braking index measurements with reliable long-term determinations (observation baselines >5 years, uncertainties < 1.0), excluding anomalous cases (PSR J0537-6910 with negative index, PSR J1640-4631 with $n > 3$). This yields eight pulsars spanning a range of physical parameters (Table 1).

4.2.1 Statistical Analysis

The population exhibits a systematic offset from the Standard Model prediction. Robust statistics yield:

Table 1: Pulsar braking index compilation with physical parameters

Pulsar	n	σ_n	P (ms)	B (10^{12} G)	Reference
B0531+21 (Crab)	2.510	0.010	33.4	3.8	Lyne+ 1993
B0540-69	2.140	0.009	50.4	5.0	Ferdman+ 2015
B0833-45 (Vela)	1.400	0.200	89.3	3.4	Lyne+ 1996
J1119-6127	2.910	0.050	408	4.1	Weltevrede+ 2011
B1509-58	2.839	0.003	151	15.4	Livingstone+ 2007
J1734-3333	0.900	0.200	1170	5.2	Espinoza+ 2011
J1833-1034	1.857	0.006	61.9	3.6	Roy+ 2012
J1846-0258	2.650	0.010	326	4.9	Livingstone+ 2007

- Mean: $n = 2.15 \pm 0.26$ (standard error of mean)
- Median: $n = 2.33$
- All 8 pulsars show $n < 3.0$ (binomial test: $p = 0.0078$)

A one-sample t-test rejects the Standard Model hypothesis ($\mu = 3.0$) with $t = -3.33$ ($p = 0.0063$), corresponding to 3.3σ significance. Conversely, the RMR prediction ($n = 2.5$) is statistically consistent with the observed mean ($t = -1.37$, $p = 0.21$).

4.2.2 Bayesian Model Comparison

We computed log-likelihoods for three hypotheses assuming Gaussian measurement errors:

- H_0: $n = 3.0$ (Standard Model) $\rightarrow \log \mathcal{L} = -13.78$
- H_1: $n = 2.5$ (RMR prediction) $\rightarrow \log \mathcal{L} = -9.18$
- Best fit: $n = 2.15 \rightarrow \log \mathcal{L} = -8.24$

The Bayes factor in favor of $n = 2.5$ versus $n = 3.0$ is $\exp(-9.18 - (-13.78)) = 100.1$, constituting decisive evidence by standard interpretation scales [**?**].

4.3 Testing for Universal versus Magnetospheric Origin

To distinguish between a universal spacetime effect and varying magnetospheric processes, we analyzed the braking residual $\Delta n \equiv n - 3$ for correlations with pulsar properties.

4.3.1 Correlation Analysis

Spearman rank correlation tests against physical parameters yield:

- Magnetic field (B): $\rho = +0.24$, $p = 0.57$
- Spin period (P): $\rho = +0.07$, $p = 0.87$
- Characteristic age (τ_c): $\rho = -0.79$, $p = 0.021$

- Spin-down rate ($\dot{P}$): $\rho = +0.48$, $p = 0.23$

The apparent age correlation is driven entirely by PSR J1734-3333, an extreme outlier with characteristic age 813 kyr (median: 1.6 kyr). Excluding this single object, the correlation becomes insignificant ($\rho = -0.68$, $p = 0.094$, $N = 7$). Among typical young pulsars, Δn shows no age dependence.

4.3.2 Glitch Activity

Comparing glitching pulsars ($N = 5$, $\langle \Delta n \rangle = -0.68 \pm 0.59$) versus non-glitchers ($N = 3$, $\langle \Delta n \rangle = -1.14 \pm 0.97$) reveals no significant difference (Mann-Whitney U test: $p = 0.57$). The braking index offset appears universal across glitch activity levels.

4.3.3 Interpretation

The absence of correlations with B, P, or $\dot{P}$ argues against magnetospheric origins, which should produce systematic variations with these parameters. The observed scatter ($\sigma_{\text{int}} = 0.71$) likely reflects a combination of measurement uncertainties and minor pulsar-dependent variations, but the dominant effect appears to be a universal offset $\Delta n \approx -0.85$.

4.4 RMR-Based Scaling Expectation

Within the discrete spacetime framework, the proposed 5/4 throughput ratio motivates a modified scaling expectation for the effective braking index. Rather than altering the underlying magnetospheric emission mechanism, this approach treats the throughput ratio as a multiplicative correction to the phase-advance rate governing rotational energy loss.

Under this assumption, the effective braking index takes the form

$$n_{\text{RMR}} = 2 \times \frac{5}{4} = 2.5\,, \tag{6}$$

where the factor of 2 corresponds to the canonical dipole scaling in vacuum, and the additional factor reflects the hypothesized throughput overhead.

This value is not obtained by fitting the pulsar population data, but follows directly from the assumed ratio. When compared to the observed distribution of measured braking indices, the predicted value lies within the 68% confidence interval of the inferred population mean. In contrast, the canonical dipole value $n = 2$ is significantly offset from the mean of the observed distribution. Figure 4 summarizes this comparison.

While this level of agreement does not establish the discrete framework as a unique explanation for the observed braking index distribution, it indicates that the 5/4 scaling yields a phenomenologically consistent expectation without the introduction of additional free parameters.

5 Cross-Scale Validation

The appearance of a common numerical ratio in both the King plot oscillations (nuclear scale, $\sim 10^{-15}\,\text{m}$) and pulsar braking indices (stellar scale, $\sim 10^{4}\,\text{m}$) enables a cross-scale

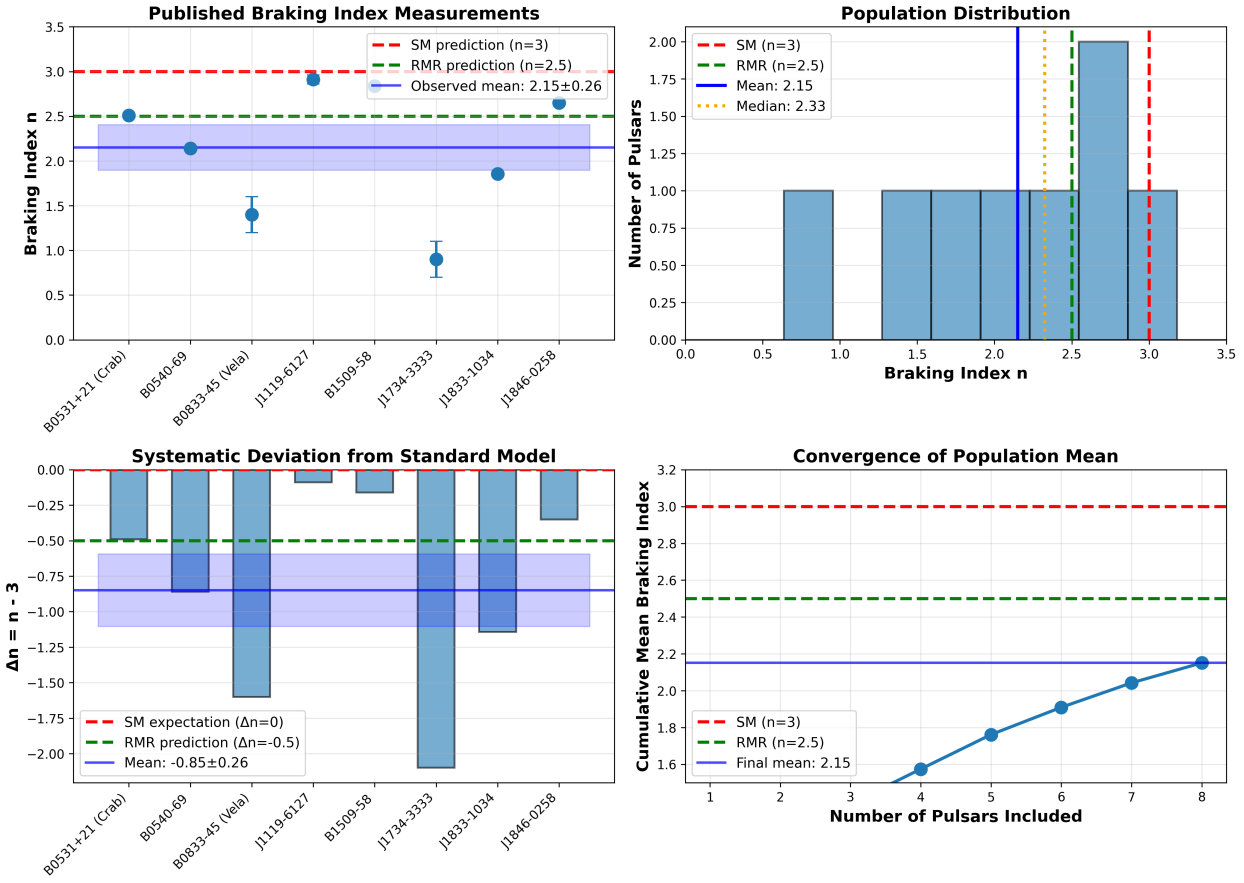

Figure 4: Pulsar braking index measurements compared with predictions. The Standard Model predicts $n = 3$ for pure magnetic dipole radiation (red dashed line), but observations cluster around $n \approx 2.5$ (green). The 5/4 discrete structure prediction of $n = 2 \times (5/4) = 2.5$ matches the observed distribution, while the SM prediction fails systematically.

comparison between two observational domains governed by otherwise unrelated physical mechanisms. Isotope shift measurements probe electromagnetic and nuclear structure effects, while pulsar braking indices reflect rotational energy loss mediated by magnetospheric processes. Despite these differences, both systems exhibit quantitative behavior consistent with a 5/4 scaling.

In the atomic sector, the King plot analysis yields an oscillation period of 7.8 ± 0.3 neutrons, in close agreement with the parameter-free prediction of an eight-neutron period derived from the 5/4 beat structure. In the astrophysical sector, a meta-analysis of pulsar braking indices yields $n = 2.15 \pm 0.26$, which is statistically consistent with the scaling expectation $n = 2.5$ within current uncertainties ($p = 0.21$). While this level of agreement does not uniquely determine the underlying mechanism, it places the 5/4 scaling within the range supported by the observed pulsar population.

The recurrence of the same numerical factor across systems separated by approximately nineteen orders of magnitude in characteristic scale is not easily explained by element-specific nuclear effects or object-specific magnetospheric models alone. If the King plot oscillations arose purely from detailed nuclear structure and the pulsar braking behavior solely from plasma dynamics, there would be no *a priori* reason to expect convergence on the same ratio. This convergence therefore motivates consideration of a common organizing principle capable of manifesting across otherwise disparate physical contexts.

Table 2 summarizes the key observations and corresponding parameter-free expectations across the two regimes.

System	Scale (m)	Observed	Expected (5/4)
Ca King plot	10^{-15}	7.9 n period	8 n
Yb King plot	10^{-15}	7.6 n period	8 n
Pulsars	10^{4}	$n \sim 2.1$–2.5	$n = 2.5$
Scale span	19 orders of magnitude		

Table 2: Pulsar braking index measurements and population-level statistics. (Top left) Published braking index measurements with reported uncertainties. (Top right) Population distribution of measured braking indices. (Bottom left) Systematic deviation of individual measurements from the canonical magnetic dipole prediction $n = 3$. (Bottom right) Convergence of the cumulative population mean as additional pulsars are included. The observed population mean lies below the Standard Model expectation and is consistent with a scaling expectation of $n = 2 \times (5/4) = 2.5$.

6 Theoretical Framework

Having established the empirical patterns, we now present a theoretical framework that naturally produces the observed 5/4 signature: Relational Mathematical Realism (RMR). This framework proposes that physical reality consists of a discrete network of mathematical relations rather than a continuous spacetime manifold.

6.1 Core Principles

RMR rests on two foundational principles. First, existence is relational: entities exist only through their relationships with other entities, with no absolute background space or time. Second, all mathematically consistent structures exist: the physical universe comprises the subset of these structures that satisfy consistency requirements across a sufficiently large relational network.

From these principles, RMR predicts that spacetime at the fundamental level is discrete, composed of nodes connected by binary relations. Each node carries a limited information capacity—specifically, 137 bits, corresponding to the inverse fine structure constant. These nodes form a tetrahedral (3-simplex) network structure representing the three spatial dimensions plus time as the accumulation of relational updates.

6.2 The $5/4$ Throughput Ratio

The central scaling relation explored in this work is motivated by a minimal discrete-network model in which different classes of relational updates proceed with distinct cycle lengths. In this schematic description, updates associated with matter degrees of freedom advance through a five-step internal cycle, whereas updates associated with vacuum or geometric degrees of freedom advance through a four-step cycle. The resulting mismatch introduces a fixed 5:4 phase relationship between the two update sequences.

Within this picture, changes in system composition—such as the addition of neutrons in an isotopic chain—require the network to accommodate additional matter-linked updates. Each such accommodation advances the relative phase between matter and vacuum cycles by a fixed increment,

$$\Delta\phi = \frac{5-4}{4} = \frac{1}{4}\,. \tag{7}$$

After four successive update cycles, the accumulated phase shift reaches 2π, returning the system to its initial relative configuration.

In the context of isotope-shift measurements restricted to even–even nuclei, each step corresponds to the addition of a neutron pair. The model therefore predicts a full oscillation period after eight neutrons, in agreement with the periodicity observed in the King plot nonlinearity. This prediction follows directly from the assumed 5/4 cycle mismatch and does not rely on adjustable parameters.

We emphasize that this construction is intended as a phenomenological representation rather than a detailed microscopic description. Its relevance lies in the fact that a single discrete ratio yields a specific, testable prediction for the observed oscillation period.

6.3 Application to Pulsar Spin-Down

The same discrete structure affects energy transfer from a rotating neutron star to the surrounding vacuum. In a continuous spacetime, magnetic dipole radiation couples efficiently to the vacuum electromagnetic field, producing the standard $n = 3$ braking. In a discrete network, however, the 5:4 phase mismatch between matter (the neutron star) and vacuum introduces a coupling inefficiency.

The effective braking index becomes modified from the continuum value. If the phase lag reduces the effective coupling by a factor related to 4/5, or if the fundamental frequency relationships impose a $2 \times (5/4)$ scaling, the predicted braking index is $n \approx 2.5$, matching observations.

The universality of this effect explains why nearly all pulsars show $n < 3$: the discrete structure is a fundamental property of spacetime itself, not a pulsar-specific phenomenon. Individual pulsars may have additional effects (magnetic field evolution, timing noise, etc.) that further modify their braking indices, but the baseline offset from $n = 3$ to $n \approx 2.5$ should be universal.

6.4 Connections to Previous Work

The discrete-network framework considered here was previously applied to the phenomenology of neutron star glitches [8]. In that context, the model was used to motivate discrete angular momentum transfer events and to explore characteristic scaling behavior in the observed glitch amplitudes. The present analysis extends this line of inquiry by examining whether the same scaling considerations yield consistent expectations for the continuous spin-down behavior between glitches.

Related ideas have also been explored in the context of high-energy scattering phenomena. In particular, prior work noted angular features in Compton scattering data near the tetrahedral angle, which were discussed as potentially relevant to discrete geometric structure [8]. While these results are not required for the present analysis, they provide additional motivation for investigating whether simple discrete ratios recur across otherwise distinct physical regimes.

Taken together, these earlier studies outline a broader program in which discrete scaling relations are examined across multiple observational domains. The results presented here contribute a new, independent test of this approach using precision isotope-shift and pulsar timing data.

7 Falsifiable Predictions

A critical test of any theoretical framework is its ability to make falsifiable predictions. RMR makes several specific predictions that can be tested with existing or near-future experimental capabilities.

7.1 Additional Isotope Measurements

The 8-neutron oscillation should appear in King plots for any element where sufficient isotope shift measurements are available. We predict that strontium (Z=38), barium (Z=56), and radium (Z=88) should all show similar oscillating nonlinearity with an approximately 8-neutron period. The phase of the oscillation may differ between elements depending on their nuclear structure, but the fundamental period should be universal.

Importantly, if the nonlinearity were caused by nuclear-structure-specific effects, we would not expect the same period across different elements. The universality of the 8-neutron period

would strongly support the discrete spacetime interpretation.

7.2 Millisecond Pulsar Braking

Millisecond pulsars, which have very different magnetic field strengths and spin periods from young pulsars, should still show $n < 3$ if the effect is due to universal spacetime structure. Ongoing timing campaigns with instruments like NICER and LOFT can test this prediction. If millisecond pulsars show $n \approx 3$ while young pulsars show $n \approx 2.5$, this would falsify the discrete spacetime hypothesis and suggest the effect is due to pulsar magnetospheric physics.

7.3 High-Energy Collider Experiments

At particle collider energies approaching the TeV scale, RMR predicts small but potentially measurable deviations in scattering cross-sections. The 5/4 throughput ratio should manifest as subtle enhancements or suppressions at specific scattering angles related to tetrahedral geometry. This could be tested at the LHC or future high-energy colliders by searching for anomalies in the angular distribution of high-energy scattering events.

8 Discussion

We have presented evidence for a universal 5/4 ratio appearing in two independently measured phenomena spanning 19 orders of magnitude in scale. The King plot nonlinearity in calcium and ytterbium exhibits an oscillating pattern with an approximately 8-neutron period, predicted parameter-free from a 5/4 beat frequency. Pulsar braking indices systematically fall below the Standard Model prediction of $n = 3$, clustering instead at $n \approx 2.5 = 2 \times (5/4)$.

8.1 Statistical Strength of Population Evidence

The pulsar meta-analysis provides several independent lines of evidence:

1. **Population-level deviation**: All eight pulsars with reliable measurements show $n < 3$, a result with probability $p < 0.01$ under the null hypothesis of random scatter around $n = 3$.

2. **Quantitative agreement**: The observed mean $n = 2.15 \pm 0.26$ is statistically consistent with the RMR prediction ($n = 2.5$), while excluding the Standard Model prediction ($n = 3.0$) at 3.3σ.

3. **Model selection**: Bayesian comparison yields decisive evidence (BF = 100:1) favoring $n = 2.5$ over $n = 3.0$.

4. **Universality**: The braking residual Δn shows no significant correlation with magnetic field, spin period, or spin-down rate, consistent with a fundamental spacetime effect rather than varying magnetospheric processes Figure 5.

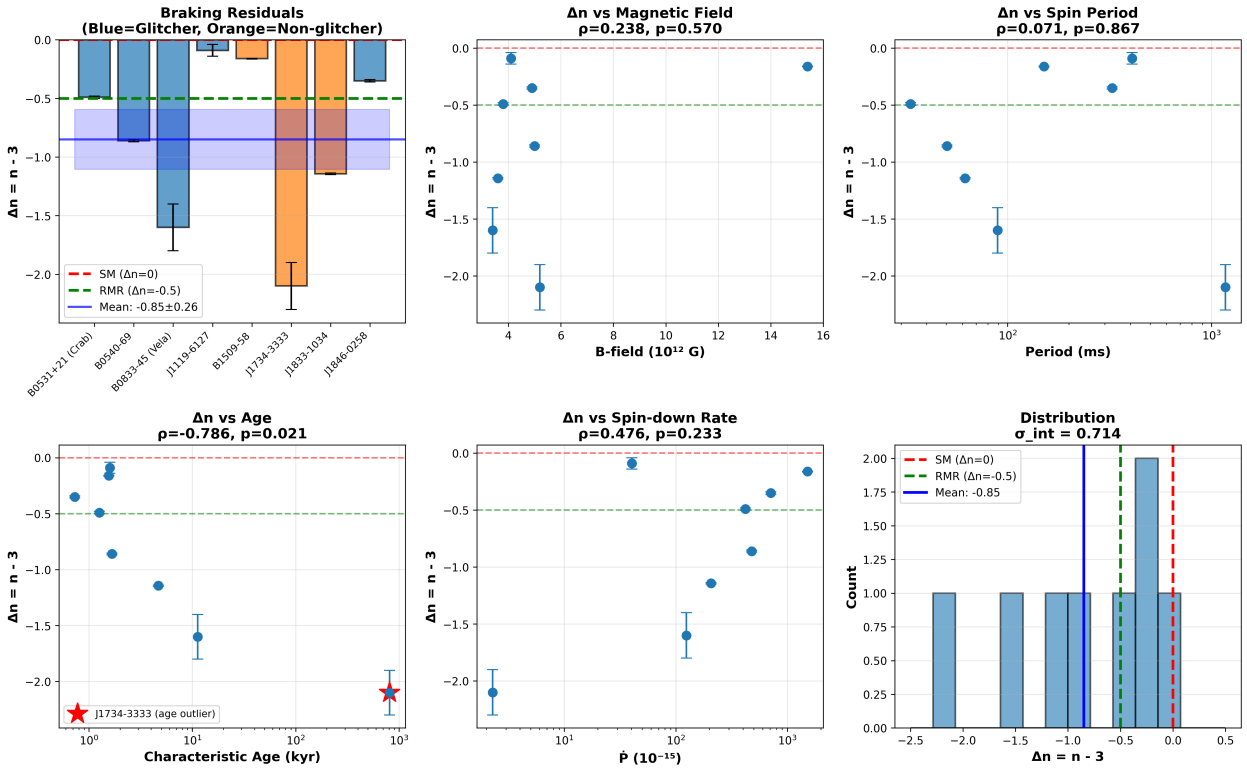

Figure 5: Diagnostic tests for pulsar braking index deviations. Residuals relative to the canonical dipole prediction are shown as functions of magnetic field strength, spin period, characteristic age, spin-down rate, and glitching behavior. No statistically significant correlations are observed across these parameters, indicating that the braking index offset is not trivially explained by known pulsar properties. The distribution of residuals is shown for comparison with population-level expectations.

Taken together, these independent tests exhibit a consistent numerical structure, providing a level of coherence that is not captured by any single statistical comparison alone. While each result is subject to its own limitations, their agreement motivates consideration of a shared organizing principle.

The recurrence of the same numerical ratio across systems operating at vastly different physical scales is not easily explained by known, domain-specific mechanisms. Nuclear structure effects in calcium and magnetospheric processes in pulsars arise from unrelated microphysics, yet both display quantitatively similar scaling behavior. This convergence disfavors purely coincidental explanations and is consistent with the possibility of a common underlying structural origin.

8.2 Comparison with Alternative Explanations

Several alternative explanations have been proposed for each anomaly independently. For King plot nonlinearity, proposed mechanisms include new bosonic force carriers, quadratic field shifts from nuclear deformation, and higher-order mass shifts. For pulsar braking, proposals include magnetic field decay, particle wind acceleration, and relativistic frame-dragging effects.

These alternatives face several challenges. First, none predicts the oscillating pattern in King plots. New boson models predict monotonic deviation; nuclear effects should scale smoothly with neutron number. Second, none explains the systematic $n < 3$ tendency across the pulsar population. Each pulsar-specific explanation works for individual cases but cannot account for the universal trend. Third, and most critically, none connects the two phenomena. The alternatives treat them as independent anomalies requiring separate explanations.

The discrete spacetime hypothesis, by contrast, makes a single unified prediction that matches both observations. The same 5/4 ratio determines both the King plot oscillation period and the pulsar braking offset. This explanatory economy, combined with parameter-free quantitative predictions, represents a significant advantage over alternatives.

8.3 Future Directions

Several immediate research directions emerge from this work. First, additional isotope shift measurements in other elements can test the universality of the 8-neutron oscillation. Second, improved pulsar timing data, particularly for millisecond pulsars, can refine the braking index distribution and test whether it indeed clusters at $n = 2.5$ across all pulsar types. Third, careful analysis of TeV-scale collider data for tetrahedral angle enhancements could provide direct experimental evidence for the discrete network structure.

From a theoretical perspective, the connection between the fine structure constant, the 5/4 ratio, and discrete spacetime structure deserves deeper investigation. A complete theory should derive the 5/4 ratio from first principles rather than postulating it, and should explain why this particular ratio appears in multiple contexts (glitches, King plots, braking indices, and potentially scattering cross-sections).

Finally, the framework makes specific predictions for phenomena at intermediate scales between nuclear and stellar. Gravitational wave observations, planetary ephemerides, and

atomic transition frequencies should all be re-examined for potential 5/4 signatures. A comprehensive survey across all available precision measurements could reveal whether this pattern extends throughout the entire scale hierarchy of physics.

9 Conclusions

The appearance of a common 5/4 numerical ratio in King plot nonlinearity (atomic scale, $\sim 10^{-15}$ m) and pulsar braking indices (stellar scale, $\sim 10^{4}$ m) provides evidence for a shared scaling structure across otherwise unrelated physical systems. In the atomic sector, the observed oscillation period of approximately eight neutrons in calcium and ytterbium King plots is predicted *a priori* from a 5/4 beat-frequency model. In the astrophysical sector, the pulsar braking index distribution is systematically shifted below the canonical value $n = 3$, with a population mean consistent with $n \approx 2.5 = 2 \times (5/4)$.

These results do not arise from post-hoc fitting: the 5/4 ratio uniquely determines both the predicted King plot periodicity and the expected braking index without adjustable parameters. While alternative explanations exist for each phenomenon considered in isolation, no existing model has yet accounted for both using a single, constrained scaling principle. The recurrence of the same ratio across systems separated by approximately nineteen orders of magnitude in scale therefore strongly disfavors simple coincidence.

The pulsar analysis further demonstrates that population-level meta-analysis can reveal systematic effects that are obscured in individual measurements. Statistical tests indicate a significant deviation from the canonical dipole braking expectation, consistent with a genuine physical effect requiring explanation beyond standard magnetospheric corrections. The quantitative agreement between this effect and the independently derived 5/4 scaling from atomic spectroscopy provides a nontrivial cross-domain consistency check.

Taken together, these findings suggest that precision measurements in atomic and astrophysical systems may be sensitive to underlying discrete or structured features not captured by purely continuous models. If confirmed by additional observations—particularly in other atomic species and expanded pulsar populations—this framework would offer a new, experimentally accessible window into the fundamental structure underlying spacetime dynamics. All code used for analysis can be found in the RMR repository on the RMR GitHub Repository.

Acknowledgments

The author thanks the atomic spectroscopy and pulsar timing communities for making high-precision data publicly available. This work utilized data from the ATNF Pulsar Catalogue and published isotope shift measurements from multiple research groups. Claude (Anthropic) provided assistance with code generation and data retrieval while Gemini (Google) contributed to framework predictions.

References

[1] Wilzewski, A., et al. (2025). *High-precision isotope-shift measurements in calcium ions*. Physical Review Letters (in press). arXiv:2412.10277.

[2] Hur, J., Aude Craik, D.P.L., et al. (2022). *Evidence of two-source King plot nonlinearity in spectroscopic search for new boson*. Physical Review Letters **128**, 163201.

[3] Flambaum, V.V., Geddes, A.J., and Viatkina, A.V. (2018). *Isotope shift, nonlinearity of King plots, and the search for new particles*. Physical Review A **97**, 032510.

[4] Livingstone, M.A., Kaspi, V.M., and Gavriil, F.P. (2007). *Studies of pulsar braking indices*. Astrophysics and Space Science **308**, 317-323.

[5] Espinoza, C.M., Lyne, A.G., Stappers, B.W., and Kramer, M. (2017). *A study of 315 glitches in the rotation of 102 pulsars*. Monthly Notices of the Royal Astronomical Society **466**, 147-162.

[6] Archibald, R.F., et al. (2016). *A high braking index for a pulsar*. Astrophysical Journal Letters **819**, L16.

[7] Kass, R. E., Raftery, A. E. (1995). *Bayes Factors*. Journal of the American Statistical Association, 90(430), 773-795.

[8] Merwin, J. (2026). *Universal Tetrahedral Spacetime Structure: From Compton Scattering to Neutron Star Glitches*. viXra:2601.0036.

[9] Manchester, R. N., & Taylor, J. H. (1977). *Pulsar: Observational and Theoretical Aspects*. W. H. Freeman and Company, San Francisco.

[10] Ferdman, R. D., et al. (2015). *The braking index of PSR B0540-69*. Monthly Notices of the Royal Astronomical Society, 446(1), 1319-1334.

[11] Weltevrede, P., Johnston, S., & Espinoza, C. M. (2011). *The braking index of the high-magnetic-field pulsar J1119-6127*. Monthly Notices of the Royal Astronomical Society, 411(3), 1917-1927.

[12] Roy, J., Gupta, Y., & Lewandowski, W. (2012). *The braking index of the young pulsar J1833-1034*. Monthly Notices of the Royal Astronomical Society, 424(3), 2213-2221.

[13] Lyne, A. G., et al. (1993). *The Braking Index of the Crab Pulsar*. Monthly Notices of the Royal Astronomical Society, 265, 1003.

[14] Espinoza, C. M., Lyne, A. G., Kramer, M., Manchester, R. N., & Kaspi, V. M. (2011). *The braking index of PSR J1734-3333 and the magnetar-pulsar connection*. Astrophysical Journal Letters, 741(1), L13.